Academic Journal of Applied Sciences
ISSN: 3105-0549 (Print), ISSN: 3105-0557 (Online) | Vol. 1, No. 2, 2026

Mineralogical Characteristics and Metallogenic Significance of Ore-Bearing Quartz Veins in Baimiaogou Molybdenum Deposit, East Qinling Molybdenum Metallogenic Belt

Xiaochen Ma *

Henan Polytechnic University, Jiaozuo Henan 454000, China

Abstract: The mineralogical analysis of ore-bearing quartz veins in molybdenum deposits is the basis for studying the formation mechanism of molybdenum deposits. This study takes the ore-bearing quartz veins of Baimiaogou molybdenum deposit in the world 's largest molybdenum metallogenic belt-East Qinling molybdenum metallogenic belt as the research object. On the basis of field geological survey and petrographic observation, combined with laser Raman spectroscopy in situ test, th e mineral composition and fabric of ore-bearing quartz veins are analyzed, and their significance for mineralization is discussed. The results show that the ore-bearing quartz veinlets mainly occur in altered andesite. The main mineral composition is quartz, grade I gray to grade I yellow, with a content of about 90% and a particle size of 0.5mm ~ 60mm. There are residual potassium feldspar cleavage and scattered argillization materials inside, and a small amount of potassium feldspar with strong argillization between quartz minerals. It shows that quartz in quartz veins is secondary quartz, which is the product of strong silicification of felsic veins, and with the enhancement of silicification, the particle size of quartz minerals gradually increases. The ore-bearing quartz veinlet contains about 5% potassium feldspar, grade I ash, and remains between quartz particles with different degrees of silicification. In the same ore-bearing quartz vein composed of secondary quartzite, with the evolution from early to late silicification, sulfide mineralization has the characteristics of transforming from pyrite and chalcopyrite to molybdenite. Molybdenite is mainly euhedral-subhedral leaf-shaped, columnar, and agglomerated with good crystallization, and a small amount is semi-euhedral-allotriomorphic grain-like structure. It is mostly associated with pyrite and chalcopyrite. It is mainly developed in potassium feldspar, which is strongly residual after strong silicification, epidotization and chloritization in ore-bearing quartz veins, and is distributed in the contact area of early and late silica fossils.

Keywords: Molybdenite, quartz veinlets, mineralogy, baimiaogou, east Qinling molybdenum metallogenic belt.

1. Introduction

The Qinling orogenic belt is located in the central part of China. It is the intersection of the North China Craton and the Yangtze plate. It records the tectonic evolution history of the central and eastern regions of China from Proterozoic to Cenozoic.

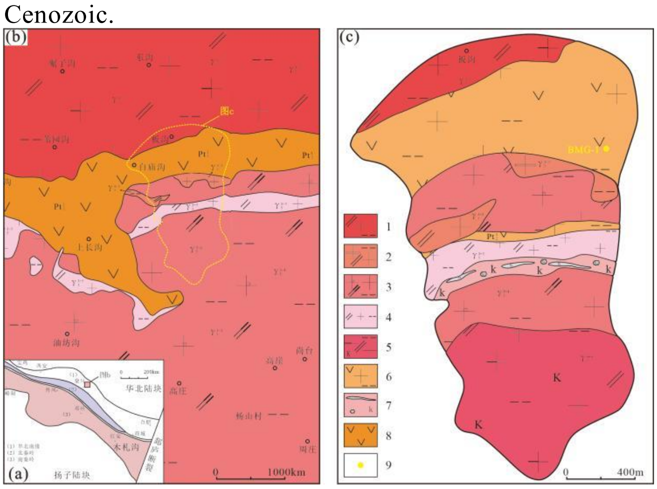

1-giant porphyritic coarse-grained granite; 2-medium coarse-grained granite; 3-medium-grained granite; 4-fine-grained granite; 5-potassium medium-grained granite; 6-meta-andesite; 7-Potassium band of local silicified lump; 8-andesite; 9-Sample location and number

Figure 1. Geological map of Baimiaogou molybdenum deposit in East Qinling molybdenum metallogenic belt

In the evolution of geological structure, the Qinling orogenic belt has experienced many tectonic movements, magmatic activities and mineralization.

The Baimiaogou molybdenum deposit is located in Luanchuan County, Luoyang City, Henan Province, China. The tectonic location is on the northwest side of the East Qinling orogenic belt. As a medium-large porphyry-skam type molybdenum deposit newly discovered in the East Qinling molybdenum metallogenic belt in recent years, the research on the deposit is very limited. Previous studies on the Baimiaogou molybdenum deposit focused on the geological characteristics and metallogenic regularity of the deposit [1-3], and the research on its petrological and mineralogical characteristics is still very lacking.

In this paper, the quartz veins containing molybdenite in the Baimiaogou molybdenum deposit in the East Qinling molybdenum metallogenic belt are taken as the research object. Based on the systematic and detailed field geological survey and petrological and mineralogical observation, the mineralogical characteristics of molybdenite-bearing quartz veins are identified by using laser Raman spectroscopy in-situ test technology, which provides guidance for regional prospecting work.

2. Reginal Geology

The East Qinling area is mainly dominated by NWW-trending and NE-trending faults. The NWW-trending faults are long-term active regional structures, which control the spatial distribution of different types of geological bodies in different periods [4]. The NE-trending fault is a large-scale fault superimposed on the NW-trending fault, which has been affected by the circum-Pacific structure since the Yanshan period [5-9]. The Precambrian crystalline basement composed of Neoarchean and Paleoproterozoic intermediate-high grade metamorphic rocks is mainly exposed in this area, as well as the Mesoproterozoic-Paleozoic volcanic-clastic-carbonate rock assemblages with different degrees of deformation and metamorphism deposited on the upper part of these crystalline basements. The Caledonian granite and Yanshanian intracontinental granite related to subduction and collision are commonly invaded in the area, among which the Yanshanian magmatic activity is the most intense [10-12].

3. Sample Collection and Test Methods

3.1. Sample Collection

The sample collected in this paper is located in the molybdenite-bearing quartz veinlet exposed in the middle of the Baimiaogou molybdenum deposit, and the sample number is BMG-1. The quartz veinlets are lenticular, about 35cm wide, and occur at the intrusive contact boundary between altered andesite and granite. The foliation of altered andesite is 274°∠69°. Molybdenite mineralization is strong in the quartz veinlet, and silicification is strong on both sides of the vein.

3.2. Testing Method

In order to analyze the mineralogical characteristics, genesis, and the relationship with the structure and structure, this paper grinds 2.5cm×5cm rock slices of molybdenite-bearing quartz veinlets, and under 2.5×10 times of single polarized light, orthogonal polarized light and reflected light, automatic scanning and photo splicing are carried out respectively to generate high-resolution images. The research-level translucent reflective polarizing microscope model is Axio Imager M2, equipped with ICCS optical system and automatic scanning stage, which can realize multi-field automatic scanning.

Raman analysis was completed in the Analysis and Testing Center of Henan Polytechnic University. The instrument is a high-resolution microscope confocal laser Raman spectroscopic imager (WITec alpha300R, Germany). The laser wavelength is 532 nm, the laser power adjustment accuracy is 0.1 mW, the minimum laser beam spot is 1 μm, the spectral resolution (full spectrum) is less than 1.5 cm^{-1}, and the spectral range is 10 cm^{-1}~ 3900 cm^{-1}.

4. Results

4.1. Petrology and Mineralogy

In the quartz veinlets containing molybdenite, the main mineral composition is quartz, which is grade I gray to grade I yellow, with a content of about 90% and a particle size of about 0.5mm-60mm.There are residual K-feldspar cleavage and scattered argillization materials in the interior, and a small amount of strongly argillized K-feldspar remains between quartz minerals. Obviously, the quartz vein should be composed of secondary quartzite, which is the product of strong silicification of felsic veins. With the enhancement of silicification, the particle size of quartz minerals tends to increase gradually (Figs. 2a-b). K-feldspar is grade I ash, with a content of 5 %. It is residual between quartz particles with different degrees of silicification. Brown mud particles are common in K-feldspar particles.

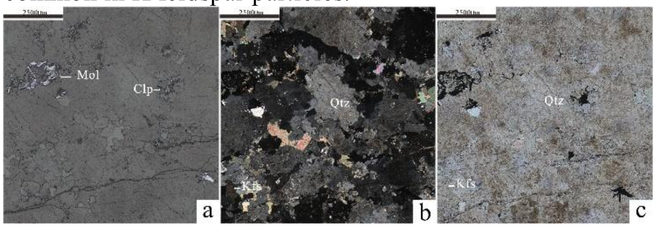

a-the characteristics of a-nonmetallic minerals under single polarization; b-nonmetallic mineral characteristics under orthogonal polarized light; characteristics of c-metallic minerals under reflected light Qtz-quartz; Kfs-potassium feldspar; mol-molybdenite; clp-chalcopyrite

Figure 2. Mineralogical characteristics of ore-bearing quartz veinlets in Baimiaogou Mo deposit, East Qinling Molybdenum Metallogenic Belt (Sample No. BMG-1)

In the same quartz vein composed of secondary quartzite, with the evolution from early to late silicification, sulfide mineralization has the characteristics of transforming from pyrite and chalcopyrite to molybdenite. Molybdenite can be developed in the residual potassium feldspar after strong silicification in quartz veins, and epidotization and chloritization are strong.

In the contact area of early and late quartz, molybdenite is mainly euhedral-subhedral leaf-like, columnar, agglomerated, radial or vein-like with better crystallization, and a small amount is semi-automorphic-allotriomorphic grain-like structure, which is mostly associated with pyrite and chalcopyrite, and is related to epidotization.

4.2. Laser Raman Spectrometry

In order to further determine the mineral type, laser Raman analysis was performed on metal and non-metal minerals with different optical characteristics in ore-bearing quartz veins (Fig.3, Fig.4).

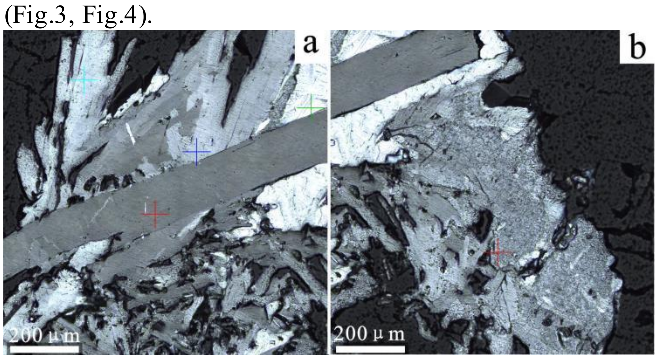

a-Early molybdenite; b-Late molybdenite

Figure 3. Laser Raman spectroscopy test point of ore-bearing quartz veinlet molybdenite in Baimiaogou molybdenum deposit of East Qinling molybdenum metallogenic belt (sample No. BMG-1)

Fig. 3 is the microscopic characteristics of molybdenite with different optical characteristics, shapes and stages in the quartz veinlet. It can be clearly seen that there are five formation stages of molybdenite in the quartz veinlet. From late to early, it is in turn the molybdenite referred to by the red cross of Fig. a, the molybdenite referred to by the blue cross of Fig. a, the molybdenite referred to by the blue-green cross of Fig. a, the molybdenite referred to by the green cross of Fig. a and the molybdenite referred to by the red cross of Fig. b.

Although the optical characteristics and morphology of the molybdenite formed in these five stages are very different, the laser Raman spectroscopy test shows that there is no significant difference in its material composition (Fig. 3).

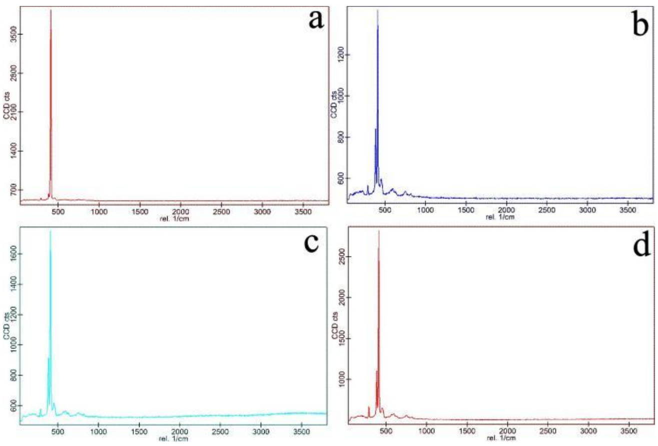

a-Figure 3a red cross-wire molybdenite Raman shift; b-Fig.3a Blue Cross Molybdenite Raman shift; c-Figure 3a blue-green cross-wire molybdenite Raman shift; d-Fig. 3b Raman shift of red cross molybdenite

Figure 4. Laser Raman shift of molybdenite in different stages of molybdenite-bearing quartz veins in Baimiaogou Mo deposit, East Qinling Molybdenum Metallogenic Belt (Sample No. BMG-1)

In addition to quartz, potassium feldspar, sericite, epidote, chlorite, non-metallic minerals also have orthoclase and grossular (Fig.5, Fig.6).

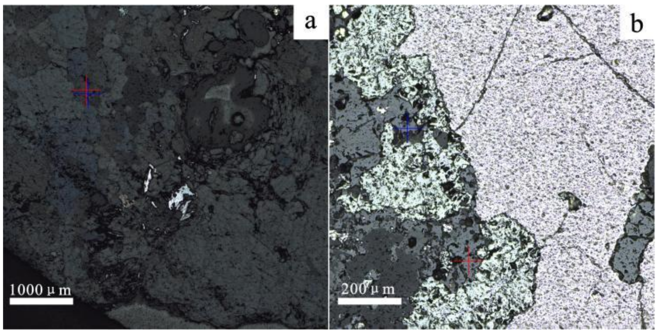

Figure 5. Laser Raman spectroscopy test points of non-metallic minerals in molybdenite-bearing quartz veins of the Baimiaogou molybdenum deposit in the East Qinling molybdenum metallogenic belt (sample No. BMG-1)

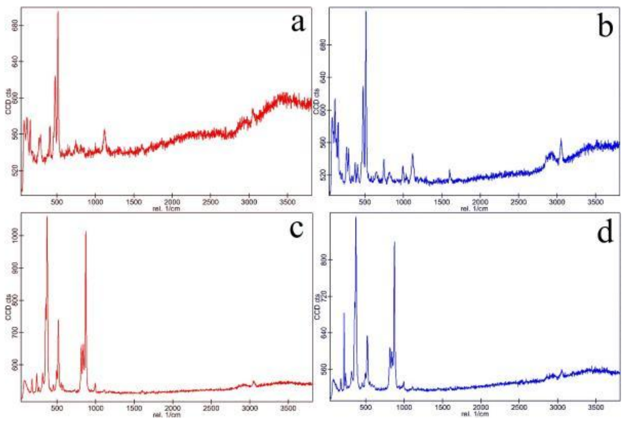

a, b-Laser Raman spectral shift of syenite; c, d-laser Raman spectral shift of grossular

Figure 6. Laser Raman spectroscopic shift of non-metallic minerals in molybdenite-bearing quartz veins of Baimiaogou Mo deposit, East Qinling Molybdenum Metallogenic Belt (Sample No.: BMG-1)

5. Discussion

5.1. Hygrothermal Process

The hydrothermal alteration of the beds in the eastern Qinling molybdenum metallogenic belt is mainly silicification, potassic alteration, sericitization and propylitization, and presents the characteristics of the transition from early potassic alteration to silicification, sericitization, epidotization and late propylitization [13-15].

The early high temperature stage is dominated by magmatic fluid, and the hydrothermal components are enriched in K^+, Si^{4+}, $Cl^-$and metal complexes (Chen et al., 2007; Chen et al., 2009), corresponding to potassium silicate alteration, is dominated by potassium feldspar-biotite-quartz mineral assemblage.

The middle-high temperature stage is dominated by the mineral assemblage of quartz-sericite-epidote-molybdenite. The hydrothermal fluid is rich in H^+, K^+ and poor in Ca^{2+}, Mg^{2+}, which is weakly acidic [13-15]. At the same time of sericitization, Fe^{2+} and Mg^{2+} are released. Sulfate can be reduced to sulfide under reducing conditions, and combined with iron and copper to form pyrite and chalcopyrite.

The migration form of Mo is mainly oxychloride (such as MoO_2Cl_2). With the decrease of fluid salinity, temperature and pressure, the increase of pH value can lead to the decomposition of molybdenum complex, promote the conversion of Mo^{6+}→Mo^{4+}, and combine with $S^{2-}$to form molybdenite (MoS2).

In the subsequent hydrothermal stage, with the further decrease of temperature, with the participation of Fe^{2+} and Mg^{2+}, propylitization of chlorite, epidote, albite and calcite mineral assemblages occurred.

When the temperature is lower than 375°C, the siliceous will precipitate during the quasi-isobaric cooling process [16], and the solubility will decrease with the decrease of temperature and pressure [17]. Silicification can continue to occur throughout the hydrothermal process.

5.2. Structural Factors

The ore-bearing quartz veins obliquely intersected with andesite foliation should be veins in a series of tension fissures (T faults) produced by the ore-forming hydrothermal fluid filling in the strike-slip process under overpressure. Microscopically, the tension fissures produced by this strike-slip effect are also obvious. The sericite formed at the same time with molybdenite mineralization is distributed along the contact boundary between granite and andesite. The wedge-shaped space and its tip at the boundary are filled with larger-sized sericite minerals and associated with molybdenite. This part should obviously be the tension fissures (T faults) caused by strike-slip action, and the sharp angle between these tension fissures and the strike-slip boundary indicates the nature of left-lateral strike-slip.

The minerals filled in the above-mentioned tension fissures can produce rapid crystallization due to the sudden decrease of pressure, which leads to the veins filled in the tension fissures have higher rock mechanical strength than the surrounding rock [18-20]. After the overpressure is released, the stress property is transformed into compression and torsion. Under the action of progressive deformation and shear, these ore-bearing veins with high rock mechanical strength obliquely intersecting with andesite foliation can be transformed into intestines.

6. Conclusion

(1) In the molybdenite-bearing quartz veins of the Baimiaogou molybdenum deposit in the East Qinling molybdenum metallogenic belt, the metal minerals are molybdenite, pyrite and chalcopyrite, and the non-metallic minerals are quartz, potassium feldspar, sericite, chlorite and epidote.

(2) According to the optical characteristics, interpenetration relationship and crystal morphology, molybdenite can be divided into five stages of formation.

(3) Quartz veinlet is an important development position of molybdenite. Potassium feldspar residue is more common in quartz veinlets containing more molybdenite, and sericite, chlorite and epidote are developed, which is an important indicator of prospecting work.

Acknowledgements

The authors gratefully acknowledge the financial support from Key R & D projects in Henan Province (231111320700).

References

[1] Archaean lithosphere, Sino-Korean craton, China [J]. Geological Society, London, Special Publications, 1993, 76(1): 71-81.

[2] Aubry J, Passelègue F X, Escartín J, et al. Fault stability across the seismogenic zone [J]. Journal of Geophysical Research: Solid Earth, 2020, 125(8): e2020JB019670.

[3] Udétat A. Source and evolution of molybdenum in the porphyry Mo (–Nb) deposit at Cave Peak, Texas [J]. Journal of Petrology, 2010, 51(8): 1739-1760.

[4] Audétat A. Compositional evolution and formation conditions of magmas and fluids related to porphyry Mo mineralization at Climax, Colorado [J]. Journal of Petrology, 2015, 56(8): 1519-1546.

[5] Audétat A, Li W. The genesis of Climax-type porphyry Mo deposits: Insights from fluid inclusions and melt inclusions [J]. Ore Geology Reviews, 2017, 88: 436-460.

[6] Annen C, Blundy J D, Sparks R S J. The genesis of intermediate and silicic magmas in deep crustal hot zones [J]. Journal of Petrology, 2006, 47(3): 505-539.

[7] Bachmann O, Huber C. Silicic magma reservoirs in the Earth's crust [J]. American Mineralogist, 2016, 101(11): 2377-2404.

[8] Bachmann O, Bergantz G W. Rejuvenation of the Fish Canyon magma body: A window into the evolution of large-volume silicic magma systems [J]. Geology, 2003, 31(9): 789-792.

[9] Bachmann O, Bergantz G W. Gas percolation in upper-crustal silicic crystal mushes as a mechanism for upward heat advection and rejuvenation of near-solidus magma bodies [J]. Journal of Volcanology and Geothermal research, 2006, 149(1-2): 85-102.

[10] Bachmann O, Bergantz G W. Deciphering magma chamber dynamics from styles of compositional zoning in large silicic ash flow sheets [J]. Reviews in Mineralogy and Geochemistry, 2008, 69(1): 651-674.

[11] Bachmann O, Deering C D, Lipman P W, et al. Building zoned ignimbrites by recycling silicic cumulates: insight from the 1,000 km3 Carpenter Ridge Tuff, CO [J]. Contributions to Mineralogy and Petrology, 2014, 167(6): 1025.

[12] Bai T B, Van Groos A F K. The distribution of Na, K, Rb, Sr, Al, Ge, Cu, W, Mo, La, and Ce between granitic melts and coexisting aqueous fluids [J]. Geochimica et Cosmochimica Acta, 1999, 63(7-8): 1117-1131.

[13] Bacon C R, Macdonald R, Smith R L, et al. Pleistocene high-silica rhyolites of the coso volcanic field, inyo county, california [J]. Journal of Geophysical Research: Solid Earth, 1981, 86(B11): 10223-10241.

[14] Bacon C R. Crystallization of accessory phases in magmas by local saturation adjacent to phenocrysts [J]. Geochimica et Cosmochimica Acta, 1989, 53(5): 1055-1066.

[15] Barboni M, Schoene B. Short eruption window revealed by absolute crystal growth rates in a granitic magma [J]. Nature Geoscience, 2014, 7(7): 524-528.

[16] Belousova E A, Griffin W L, O'Reilly S Y, 2006. Zircon crystal morphology, trace element signatures and Hf isotope composition as a tool for petrogenetic modelling: examples from eastern australian granitoids [J]. Journal of Petrology, 47(2): 329-353.

[17] Brimhall G H, Crerar D A. Ore fluids: magmatic to supergene [M]. Thermodynamic Modeling of Geologic Materials. De Gruyter, 1987: 235-322.

[18] Buddington A F. Granite emplacement with special reference to North America [J]. Geological Society of America Bulletin, 1959, 70(6): 671-747.

[19] Brown M. Crustal melting and melt extraction, ascent and emplacement in orogens: mechanisms and consequences [J]. Journal of the Geological Society, 2007, 164(4): 709-730.

[20] Chen Y J, Wang P, Li N, et al. The collision-type porphyry Mo deposits in Dabie Shan, China [J]. Ore Geology Reviews, 2017a, 81: 405-430.